Dalton Transactions

Accepted Manuscript

ROYAL SOCIETY OF CHEMISTRY

www.rsc.org/dalton

Journal Name
Dalton Transactions

Cite this: DOI: 10.1039/c0xx00000x

www.rsc.org/xxxxxx

ARTICLE TYPE

Probing a highly efficient room temperature ammonia gas sensing properties of luminescent ZnO nanowires array via AAO-assisted template route

Nagesh Kumar[a], A.K. Srivastava[b], R. Nath[a], Bipin Kumar Gupta[c*] and G.D. Varma[a*]

Received (in XXX, XXX) XthXXXXXXXXX 20XX, Accepted Xth XXXXXXXXX 20XX
DOI: 10.1039/b000000x

Here, we report the facile synthesis of highly ordered luminescent ZnO nanowires array using low temperature anodic aluminium oxide (AAO) template route which can be economically produced in large scale quantity. The as-synthesized nanowires have diameters ranging from 60-70 nm and length ~11 µm. The photoluminescence spectrum reveals that the AAO/ZnO assembly has a strong green emission peak at 490 nm upon 406 nm excitation wavelength. Furthermore, the ZnO nanowires array-based gas sensor has been fabricated by a simple micromechanical technique and its NH_3 gas sensing properties have been explored thoroughly. The fabricated gas sensor exhibits excellent sensitivity and fast response to NH_3 gas at room temperature. Moreover, for 50 ppm NH_3 concentration, the observed value of sensitivity is around 68%, while the response and recovery times are 28 and 29 seconds, respectively. The present synthesis technique to produce highly ordered ZnO nanowires array and fabricated gas sensor has great potential to push the low cost gas sensing nanotechnology.

1. Introduction

Among all the nanoscale materials, the metal oxide nanostructures are extensively studied because of their potential applications in various technological areas, such as electronics, lasers, electron-field emitters, optoelectronics, biological and chemical sensors, logic devices, nanoscale memory, coating systems, superconductivity and catalysis [1-10]. Recently, many research groups have extensively investigated the various properties of metal oxide nanonstructures of different dimensions (D) and they observed that only some of these possess either d^0 (TiO_2, WO_3, Sc_2O_3, V_2O_5, CrO_3 and perovskites such as $ScTiO_3$, $LiNbO_3$) or d^{10} (ZnO, SnO_2, Cu_2O, In_2O_3) electronic configuration of cations exhibit feasible gas sensing properties [11]. Although there exist a few metal oxides with d^n ($0<n<10$) configuration of cations (NiO, VO_2, Cr_2O_3, RuO_2 etc.) which are sensitive to the environment in their vicinity, but these are structurally unstable as influenced by oxidation or reduction processes[12]. Amid the metal oxides nanostructures, ZnO is one of the most studied semiconducting materials. It possesses thermodynamically highly stable wurtzite (hexagonal close packed) crystal structure in which lattice constants c/a ~ 1.60 slightly deviates from the ideal value of hexagonal cell c/a = 1.633 due to difference between electronegativity values of Zn^{2+} and O^{2-} ions. ZnO exhibits almost all the unique properties required to make it a feasible gas sensor such as moderate direct band gap (3.37 eV), high mobility of conduction electrons, better chemical and thermal stability under ambient conditions and good activity in redox reactions [13,14]. Thus 0D, 1D, 2D and 3D nanostructure of ZnO have been extensively studied worldwide to utilize their excellent gas sensing properties in the fabrication of improved gas sensing devices at low cost. Moreover, the longer dimension of 1D ZnO nanostructures (nanotubes, nanowires and nanorods) make them suitable to contact with macroscopic world for electrical and many others physical measurements. Therefore, 1D nanostructures are more appropriate for the fabrication of nanoelectronics devices like gas sensors, electron-field emitters and logic devices etc.

In recent times, many research groups have demonstrated the excellent sensitivity, response and recovery characteristics of zinc oxide gas sensors fabricated with individual nanostructure (tube, wire and rod) [15-17]. However, the large-scale fabrication process of these sensors still suffers from intrinsic drawback of processing an individual nanostructure. To address this issue, we proposed alternative route to minimize such drawbacks by highly ordered template based aligned luminescent ZnO nanowires

array. In order to control over the material properties and developing functional devices it is necessary to synthesize nanostructures with high degree of regularity and alignment at low cost. In general, most of the reported ZnO nanostructures with different diameters and lengths are synthesized by various methods like solid-liquid-vapor process, metal-organic chemical vapor deposition, pulsed laser deposition, wet chemical methods and template-assisted methods [18-22]. Recently, AAO- template route is the most impressive way because of their low growth temperatures and good potential for large scale synthesis of ordered nanostructures [23-28].

The photoluminescent properties of ZnO has received much attention because of the ability to tune the optical properties of ZnO via tailoring its band gap (direct band gap of 3.37 eV) with higher exciton binding energy (60 meV) as compared to other semiconductor materials such as; ZnSe (22 meV), ZnS (40 meV) and GaN (25 meV) which make it suitable for short wavelength optoelectronic devices and gas sensor applications [29-32]. Typically ZnO exhibits photoluminescence characteristic in visible and UV regions, the UV emission at 370 nm is due to radiative inhalation of exciton while the green luminescence in ZnO arises due to inhalation involving intrinsic defects centers such as oxygen vacancies [33-35], interstitial oxygen [36, 37], zinc vacancies and interstitial zinc [38]. In present investigation, the interface between ZnO nanowires in the AAO creates a lot of oxygen vacancies which is responsible for strong luminescence.

The gas sensing properties of the as synthesized ZnO nanowires array-based gas sensors were investigated against NH_3, which is highly toxic but have wide-ranging commercial applications such as in chemical industries, fertilizer factories, food processing, air conditioning equipment and refrigerators as a coolant and in the manufacturing of commercial explosives (e.g., trinitrotoluene (TNT), nitroglycerin, and nitrocellulose). The natural level of NH_3 in the atmosphere is about 1-5 ppb and odor threshold is about 5 ppm. The American Conference of Governmental Industrial Hygienists (ACGIH) has assigned NH_3 a threshold limit value of 25 ppm for a normal 8 h work per day and a 40 h work per week. Therefore a system is required which can detect the presence of high as well as low concentrations of NH_3 in the environment. Various NH_3 sensors, including ZnO based sensors, have been reported so far but most of them are operated at high temperatures (up to 300 ^{0}C) to activate the adsorption and desorption processes of NH_3 which limits their use in low temperature applications [39-43]. Furthermore, low power consumption is the most important demand on the gas sensors since they work day and night. Thus, to save energy and reduce the working temperature researchers are currently looking for a smart portable NH_3 gas sensor with good response and recovery time that can be operated at room temperature.

Here, in the present work, we explore the facile synthesis of highly ordered luminescent ZnO nanowires array using low temperature anodic aluminum oxide (AAO) template method. The obtained photoluminescence spectrum exhibits strong green emission peaks at 502, 457 and 490 nm upon 406 nm excitation wavelength corresponding to pristine AAO template, ZnO nanowires and AAO/ZnO assembly, respectively. Moreover, we have also investigated the fabrication as well as gas sensing mechanism, properties including sensitivity, recovery and fast response to NH_3 gas at room temperature.

2. Experimental

2.1. Synthesis of ordered ZnO nanowires arrays

ZnO nanowires of uniform size were synthesized using anodic aluminum oxide (AAO) templates. The AAO templates having ordered nanopores of 45-50 nm diameters and thickness of 12 µm were prepared and detached from Al substrates by the method reported earlier [44]. After pore widening treatment in 6 wt%

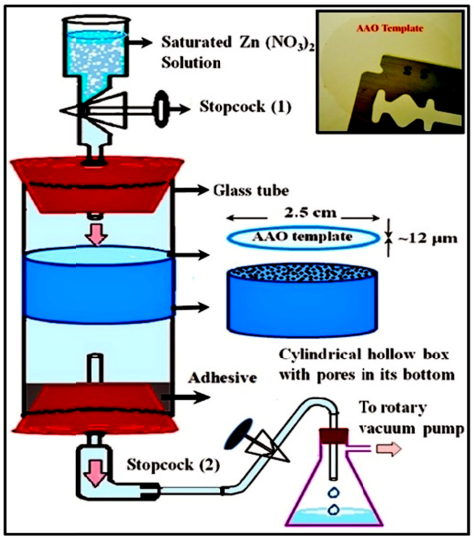

Figure. 1 Schematic diagram of the setup used for inserting solution into the pores of AAO template.

phosphoric acid solution (for 25 min. at room temperature) the template was mounted on the porous base of a hollow cylindrical

box (schematic diagram shown in Figure 1) which was inserted into the glass tube after applying a small amount of vacuum grease. The bottom end of this glass tube was connected to a vacuum flask through a thin rubber pipe and stop cock (2). The inset of Figure 1 shows the detached AAO-template supported on the razor blade. The vacuum flask in the set-up does not only prevent the solution to enter into the vacuum pump but also prevent air to enter into the glass tube. Further, the solution level inside the glass tube can also be easily controlled with the help of a stop cock (2). After attaining the desired vacuum (3–4 × 10^{-2} torr) in the system, stopcock (1) in Figure 1 was opened slowly to allow saturated zinc nitrate solution to pass over AAO-template. Stopcock (1) was closed again as soon as the solution in the container was about to finish. Due to vacuum, some solution from glass tube entered into the vacuum flask and after that stopcock (2) was closed. It should be noted that during the whole process template inside the tube remained dipped in the solution. Sometimes bubbles appear in the solution just above the template surface which prevents the solution from entering into the pores. This problem was overcome by pushing more solution into the glass tube through stopcock (1) and the system was left in this condition for approximately 8 h. Later, AAO-template was removed from the cylindrical box and kept in an electric oven at ~ 70°C for 6 h. Finally, it was annealed at 435°C for 40 h in order to obtain wurtzite ZnO nanowires. In order to collect the ordered nanowires, the annealed template was thoroughly dissolved in 0.1 M NaOH solution and the floating material was collected on a razor blade. *Prior to* FESEM *analysis* this material was dried at around 70-80°C. For TEM analysis the material collected on the razor blade was dispersed in methanol and ultrasonicated for a few seconds.

The sample was characterized by field-emission scanning electron microscope (FE-SEM, FEI QUANTA 200F), transmission electron microscope (TEM, Philips CM200 equipped with LaB_6 filament operating at 200 kV). PL spectra were taken on Edinburgh, FLSP-920, Xenon flash lamp as the source of excitation.

2.2. Fabrication of ZnO nanowires array gas sensor

In order to study the gas sensing characteristics of the as synthesized ZnO nanowires arrays, we fabricated a simple system of two electrodes as shown in section 3.3. Here two thin Cu wires were taken and the curvature at the end of each wire was reduced either by pressing or by hitting it gently. These wires were fixed on glass plate which is covered with an insulating tape, and the gap between two flat ends of the wires was adjusted to be less than 10 μm with the help of optical microscope. Using this technique we can make 2-3 such pairs of Cu wires on the same glass plate and in the inset of Figures located in section 3.3, we show a magnified "A" region of one of these glass plates. A drop of ZnO nanowires suspension in ethanol was dropped between the gap of each pair of Cu wires and an ac electric field with magnitude 15 Vpp (peak to peak) at 0.5 MHz was applied between points "1" and "2" as shown in section 3.3.

3. Results and discussion

3.1. FESEM and TEM studies of ZnO nanowires

Figure 2(a) exhibits the FESEM image of the filled and annealed AAO-template and inset shows the magnified view of "A" region. It can be seen that almost all the pores of the template are uniformly filled with the material. Figure 2(b) shows the FESEM image of annealed template after partially dissolving it in

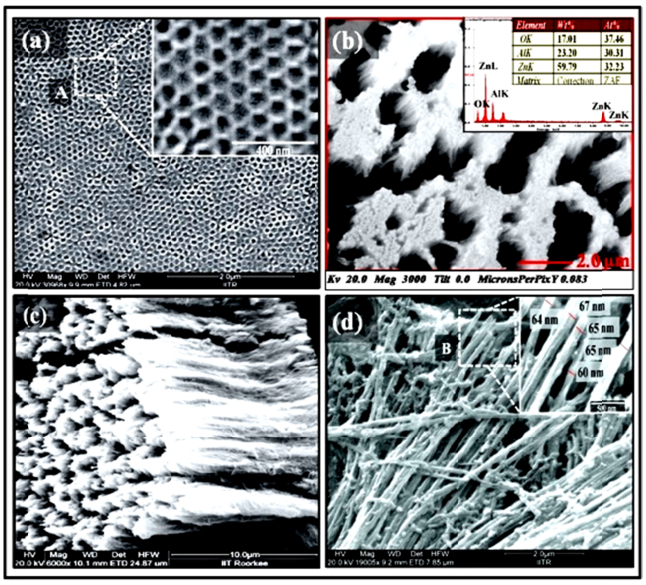

Figure 2(a) FESEM image, and inset shows magnified image of "A" region of the filled and annealed AAO template, **(b)** FESEM image of nanowires array after partially dissolving the filled and annealed AAO template in 0.1 M NaOH solution, inset shows EDX profile for the same **(c)** cross-sectional FESEM image of ZnO nanowires array and **(d)** FESEM image and inset shows magnified image of "B" region of ZnO nanowires.

0.1 M NaOH solution for ~ 20 min and inset shows EDX profile of the same. In the image, tips of the ZnO nanowires embedded in the template can be clearly seen. Figure 2(c) is the cross sectional FESEM image of ZnO nanowires array after completely dissolving the alumina template in NaOH solution. It shows that the length of the nanowires are around 11 µm. FESEM image reveals that the ZnO nanowires are uniform, dense, independent and almost parallel to each other with diameters between 60-70 nm as Figure 2(d).

TEM image, SAED pattern, HRTEM image and magnified HRTEM image of the as synthesized ZnO nanowires are shown in Figure 3 (a), (b), (c) and (d), respectively. In Figure 3(a) the TEM micrograph shows that the nanowires have smooth surface and have an average diameter of ~ 67 nm. The SAED pattern in Figure 3(b) indicates the polycrystalline nature of ZnO nanowires. All the polycrystalline rings observed in the SAED pattern are indexed with pure ZnO wurtzite phase. HRTEM in Figure 3(c) confirms the polycrystalline nature of ZnO nanowires. The Figure 3(d) corresponds to a d-spacing value of (~ 0.29 nm) which corresponds to (100) planes of ZnO without much lattice distortion.

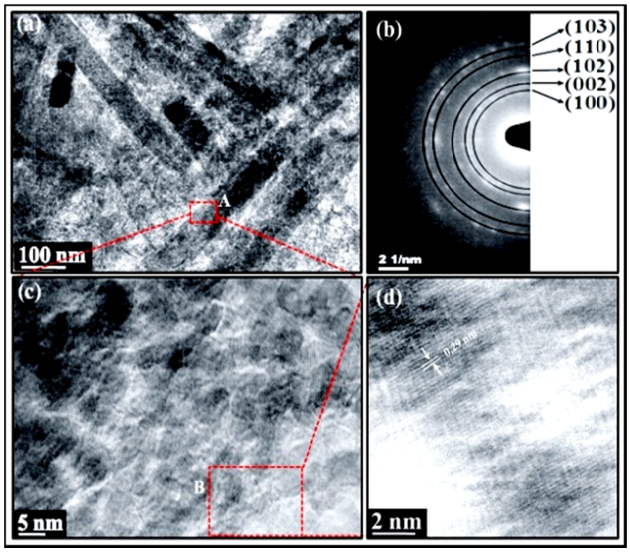

Figure 3 (a) TEM micrograph of ZnO nanowires, **(b)** Marked SAED pattern of ZnO nanowire **(c)** HRTEM image of a single ZnO wire showing interplaner spacing and **(d)** magnified HRTEM image.

3.2. Photoluminescence study of ZnO nanowires

Photoluminescence (PL) is an important tool for direct optical investigation to explore electronic band structure and surface defects analysis. It can provide useful qualitative information about the interaction of free electrons on the surface of AAO template with ZnO nanowires. Figure 4(a) exhibits the excitation spectrum of AAO/ZnO template at 490 nm emission which was evaluated by pre-scan of the AAO/ZnO template assembly in range of 200-900 nm. Figure 4(b) consists of three broad strong green emission spectra peaks at 457,502 and 490 nm upon 406 nm excitation wavelength corresponding to ZnO nanowires, pristine AAO template and AAO/ZnO assembly which are represented by curves 1, 2 and 3, respectively. Here, the emission spectrum of ZnO nanowires (curve1) was obtained after subtracting the curve 2 from curve 3 and the intensity of ZnO nanowires emission spectra (curve 1) was found **2.5 times** lower than that of AAO/ZnO assembly (curve3). The origin of defect related electron hole recombination process in ZnO nanowires has been extensively investigated; however, it remains a debatable subject of matter. Among the different mechanisms proposed to explain the visible luminance in ZnO nanowires till date, oxygen vacancies have been widely accepted as the most probable candidate [45]. In the present investigation, we have used AAO template for synthesis of aligned ZnO nanowires which introduced intrinsic defects on the surface of ZnO nanowires in order to enhance the strong green emission compared to pristine AAO as well as ZnO as shown in Figure 4 (b) [46]. The broad emission peaks in the spectra are the consequence of different types of defects existing in the samples. We proposed that AAO plays a key role in enhancing the green emission in AAO/ZnO hybrid structure. The strong interface formed during synthesis of ZnO nanowires on AAO template, which creates higher defect densities in ZnO, gives rise to higher PL intensity in comparison to pristine ZnO and pristine AAO.

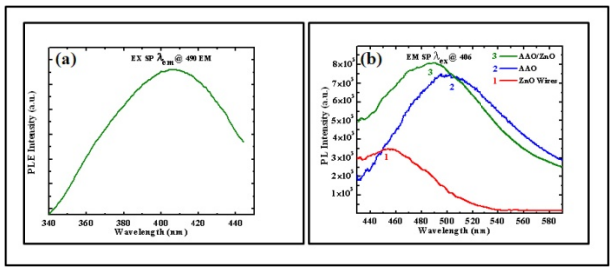

Figure 4 (a) The photoluminescence excitation spectra (PLE) of AAO/ZnO assembly, **(b)** three broad strong green emission spectra peaking at 457, 502 and 490 nm upon 406 excitation wavelength corresponding to ZnO nanowires, pristine AAO template, and AAO/ZnO assembly which are represented by curves 1, 2 and 3 respectively.

The other probable reason behind the strong luminescence in AAO/ZnO may be higher interfacial area provided by ZnO nanowires to AAO. Higher surface to volume ratio leads to higher concentration of defects induced by **AAO- template** on the ZnO nanowire surface, as a result the recombination of Vo+ from the ZnO surface and free electrons from AAO recombine strongly as compared to pristine ZnO to produce strong green emission.

3.3. V-I characteristic of nanowires

When an ac electric field with magnitude 15 Vpp (peak to peak) at 0.5 MHz was applied between points "1" and "2" (Figure 5(a)) (after putting a drop of suspension between gap of the electrodes) electric field (E) induces charge separation and the resulting polarization develops a dipole moment which aligns the nanowires parallel to the field lines. In case of non-uniform field distribution, the alignment force or the dielectrophoretic force ($F \propto \nabla|E|^2$, where ∇ is the gradient vector operator) moves the polarized structure towards the region of highest field density [47]. ZnO nanowires array trapped between the two Cu electrodes due to this dielectrophoresis process is shown in Figure 5(b).

The *V-I* characteristic of the ZnO nanowires array, trapped between the electrodes (Figure 5(b)) is shown in Figure 6(a).

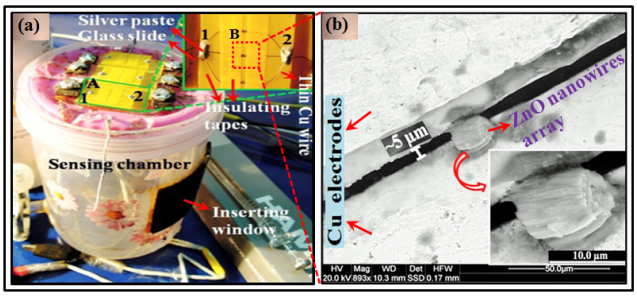

Figure 5 (a) Schematic diagram of the chamber used for gas sensing measurements and inset shows magnified "A" region of one of the glass plate which consists 3 pairs of Cu electrodes and **(b)** magnified FESEM image of "B" region which shows nanowires array kept between one pair of the two electrodes.

Cu-ZnO nanowires array, which is basically a metal-semiconductor-metal (MSM) structure, shows almost symmetric characteristics. Such MSM structure can be considered as being composed of two Schottky barriers connected back to back in series with a semiconducting material. If a barrier at both ends of the nanowires array possesses similar good quality of contacts with approximately lower barrier heights, the symmetric characteristics shall be obtained [48]. The resistance of the nanowires array is of the order of 6 GΩ at 1 V, which includes contact resistance as well. Such high resistivity is due to ZnO being a wide bandgap semiconductor (E_g = 3.3 eV) at room temperature [49].

3.4. Gas sensing properties of nanowires

For investigating room temperature gas sensing properties of the trapped ZnO nanowires array, the sensor was kept in an air tight box (volume 500 cm^3). A 1000 ppm NH_3 (Chemtron science laboratories pvt., India) was used as test gas and using the relation (Capacity of syringe used × ppm level mentioned on canister = Capacity of sensing container × required ppm level) different quantities of 1000 ppm NH_3 were inserted into the airtight sensing box through inserting window using a micro-syringe so as to yield a desired ppm concentration of NH_3. A fixed bias of 0.1 V was applied across the electrodes (points "1" and "2" in Figure 5(a)) and the change in the resistance of the sensor was measured using a pico-ammeter. Before starting the measurement for every next NH_3 concentration the test gas in sensing chamber is pumped out using a vacuum pump so that sensor recovers its initial resistance value. Figure 6(b) shows the response and recovery curves (in terms of resistance) of the ZnO nanowires array upon exposure to 10, 15, 25, 50, 75, 100 and 150 ppm NH_3 at room temperature. These curves show that the change in the resistance sensibly depends on the NH_3 concentration and it increases with increase in the value of NH_3 concentration. The % response (S) of this sensor for 50 ppm NH_3 is shown in Figure 6(c). The % response (S) of a sensor is defined as $\left|(R_a\text{-}R_g)/R_a\right| \times 100$, where R_a and R_g are resistances of the sensor in air and gas, respectively. Figure 6(c) shows that the response and recovery times (defined as the time required to reach 90% of the saturation value) of the sensor when exposed to 50 ppm NH_3 concentration are ~28 s and ~29 s, respectively. The response time of the sensor decreases with an increase in the gas concentration while the recovery time increases with an increase in gas concentration. This behavior of the sensor is shown in Figure 6(d).

NH_3 concentration versus % response of the sensor is shown in Figure 7. It can be seen that the % response increases almost linearly with increase in NH_3 concentration up to75 ppm and above 75 ppm, % response increases slowly with the increase in NH_3 concentration.

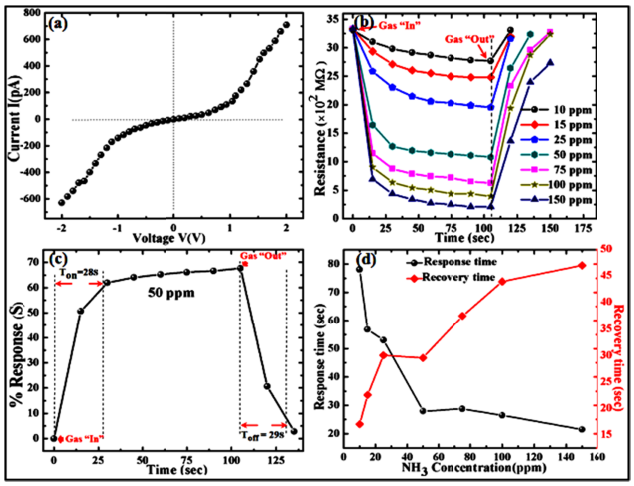

Figure 6 (a) *V-I* curve of ZnO nanowires array kept between the two electrodes, **(b)** variation in the resistance of ZnO nanowires array with time when exposed to different concentrations of NH_3 at room temperature, **(c)** response curve of the sensor for 50 ppm NH_3 and the curve is utilized to calculate the response and recovery times **(d)** response and recovery times of the sensor with respect to the NH_3 concentration.

Linear response of the sensor up to 75 ppm shows a power law dependence of the % response(S) on the gas concentration (C), i.e, $S = AC^{\alpha}$, where A is a constant [50, 51]. The reason behind the power law dependence is associated with the interaction or adsorption of NH_3 molecules on the sensing surface and with the change of surface potential. Power law fit to the linear portion of the response (S) and concentration (C) curve is shown in the inset in Figure7. The fitting data reveals that the value of α is about 0.75 which is in agreement with the predictions of rational value (1 or 1/2) for the power law exponent.

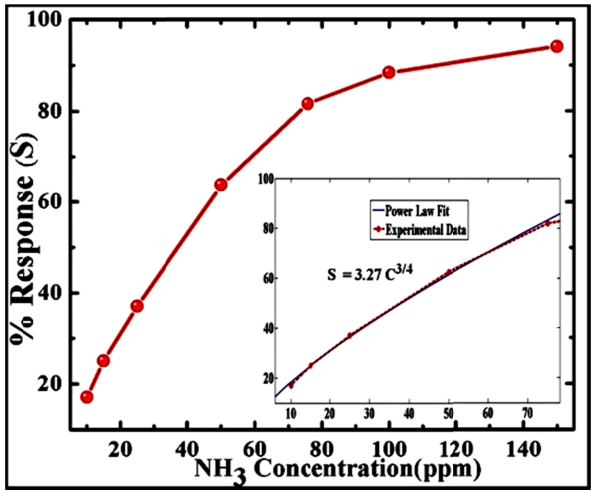

Figure 7 NH_3 concentration Vs response and inset shows the power law fit to the linear portion of the curve.

Most metal-oxide-semiconductor gas sensors work on the principle of change in the conductance of the sensing materials due to the interaction between the gas species and the adsorbed oxygen ions (O_2^-, $O^-$and O^{2-}). Initially, when ZnO nanowire sensor is placed in open atmosphere, the adsorbed oxygen ions (O_2^-, $O^-$and O^{2-}) extract electrons from the conduction band forming a depletion region which reduces the conducting width of ZnO wires and increases the potential barrier of the contacts between the nanowires and hence increases the resistance of the sensor. The nature and concentration of chemisorbed oxygen species strongly depend on temperature. O_2^- is commonly chemisorbed at lower temperatures (<100 ^{0}C). At higher temperatures O^- and O^{2-} are usually chemisorbed while O_2^- disappears rapidly [52]. On exposure to NH_3 at room temperature O_2^- species at sensor surface interacts with NH_3 resulting in release of electrons. The reaction kinetics can be described as follows:

$$O_2(gas) \rightarrow O_2(ads) \quad (1)$$

$$O_2(ads) + e^- \rightarrow O_2^-(ads) \quad (2)$$

$$4NH_3 + 5O_2^- \rightarrow 6H_2O + 4NO + 5e^- \quad (3)$$

Thus, the trapped electrons are released back into the ZnO conduction band leading to increase in the carrier concentration of the ZnO active layer. Thus the sensor resistance decreases upon exposure to NH_3 gas, as shown in Figure 6(b).

The sensing properties of a sensor greatly depend upon the microstructural features of the sensing material, such as geometry, aspect-ratio and the connectivity among the nanostructures (wires, grains etc). The sensing material in this sensor is ZnO nanowires which are vertically aligned and in contact with each other. These nanowires are in the form of bundle and almost parallel to the gap between the electrodes. For ZnO wire in air the Debye length (the distance over which a local electric field affects the distribution of free charge carriers) is 30 nm which is comparable to the radius of our synthesized ZnO

nanowires (~34 nm) [53, 54]. This implies that the nanowire is almost depleted and the surface depletion will greatly influence the density and mobility of the electrons in the nanowire. The sensing mechanism of an individual ZnO nanowire is shown in Figure 8.

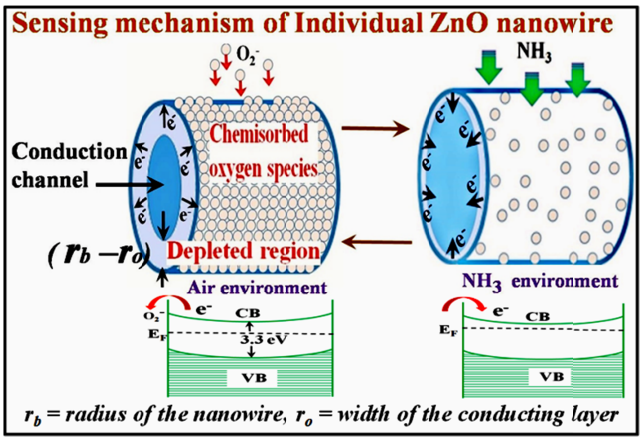

Figure 8 sensing mechanism of an individual ZnO nanowire and energy level diagrams of the wire in air as well as in NH_3 environment.

Since here Debye length is comparable to the radius of the nanowire therefore in air environment the adsorption of oxygen species (electron acceptor) on the surface of the nanowire shifts the Fermi level away from the conduction band where as in NH_3 environment due to the presence of oxygen vacancies the ZnO nanowire behave as n-type semiconductor. In nanowires array, the nanowires are in contact with each other therefore depletion layer will effectively modify the potential barrier at contact between the wires. On considering above facts and using neck-grain boundary control model total resistance (R) of the nanowires array can be written as [54, 55]:

$$R = R_N + R_C \quad (4)$$

Where R_N is the bulk resistance of the ZnO nanowires array and R_C is the contact resistance. On substituting the values of R_N and R_C in Eq. (4) total resistance,

$$R = \frac{L}{n\pi e[\mu_b n_b r_0^2 + n_d \mu_d (r_b^2 - r_0^2)]} + R_0 \exp\left\{-\frac{e\Delta V_b}{\kappa_B T}\right\} \quad (5)$$

here L is the length of nanowires, n is number of parallel ZnO nanowires in the array, e is the charge of electron, μ_b is the electron mobility in the neutral layer, μ_d is the electron mobility in the depleted region, n_b is the free electron density in the nanowire, n_d is the free electron density in the depleted region, r_o is the width of conducting layer, r_b is the radius of nanowire, R_0 is a constant term which depends on air resistance and other parameters, k_B is the Boltzmann's constant, T is the absolute temperature and ΔV_b is the change in contact potential barrier, i.e. potential in air minus that in ammonia.

The contact resistance of the ZnO nanowires is controlled by the interwire barriers at the contact and this potential barrier is the key factor in controlling the total resistance of the sensor (R) and thus influences the transport of electrons between the wires. When the sensor is exposed to NH_3, due to the exchange of charge carriers between ammonia molecules and the adsorbed oxygen species the depletion width decreases. This will cause the decrease in barrier potential width and height at the contacts. Thus ΔV_b increases and the total resistance (R) of the nanowires sensor decreases. The % response of a sensor depends on change in resistance (ΔR) upon exposure to test gas. On increasing the gas concentration, ΔV_b increases as a consequence sensor resistance decreases and hence the response of the sensor increases. On increasing NH_3 concentrations continuously the contact potential barriers ΔV_b rapidly decreases and the slope of the response curve decreases with it (Figure7). The reason behind this is the decreased possibility of the charge sharing between the ammonia and adsorbed oxygen due to reduction in the concentration of adsorbed oxygen species at the surface of the nanowire [56]. Thus sensor saturates at higher concentrations as shown in Figure 7.

The bi-functional optical and gas sensing properties of this material creates new avenues for optoelectronic and gas sensing applications.

4. Conclusion

In summary, we have successfully synthesized luminescent ZnO nanowires and fabricated a gas sensor by a simple cost effective technique in which empty pores of the commercial **AAO-template** were filled with the material by vacuum sucking technique. The photoluminescence spectrum reveals that the AAO/ZnO assembly has a strong green emission peaking at 490 nm upon 406 nm excitation wavelength. The AAO/ZnO has higher luminescence intensity compare to pristine ZnO due to its high surface to volume ratio. In order to study the

sensing characteristic of the as synthesized nanowires array a simple sensing system were made using a micromechanical technique. The sensor shows good response to NH_3 atmosphere at room temperature. We believe that these simple and cost effective techniques can be extended to synthesize nanowire arrays of other metal/metal oxides too and may be helpful in studying their sensing properties forwards various gases at room temperature.

Acknowledgements

The authors are grateful to Dr. S. K. Gupta (B.A.R.C.) for helpful discussion. The financial support from BRNS (DAE) is highly acknowledged. Mr. Nagesh Kumar acknowledges the financial support from CSIR, New Delhi, India, under Senior Research Fellowship (2012-13).

Notes and references

[a]*Department of Physics and Centre of Nanotechnology, Indian Institute of Technology Roorkee, Roorkee-247667, India*

[b]*Indus Synchrotrons Utilization Division, Raja Ramanna Centre for Advanced Technology, Indore- 452013, India*

[c]*National Physical Laboratory (CSIR) Dr K S Krishnan Road, New Delhi 110012 (India)*

** Email: gdvarfph@iitr.ernet.in, bipinbhu@yahoo.com, Fax: +91 1332 273560*

[1] R. Kumar, N. Khare, Thin Solid Films 516 (2008)1302 -07.

[2] H. Yan, J. Johnson, M. Law, R. He, K. Knutsen, J.R. McKinney, J. Pham, R. Saykally, P. Yang, Adv. Mater. 15 (2003) 907-910.

[3] J. Singh, S.S. Patil, M.A. More, D.S. Joag, R.S. Tiwari, O.N. Srivastava, Appl. Surf. Sci. 256 (2010) 6157-6163.

[4] T. Yu, F.-C. Cheong, C.-H. Sow, Nanotechnology 15 (2004) 1732-1736.

[5]Y. Li, P.-C. Hsu, S.-M. Chen, Sens. Actuators B: Chem. 174 (2012) 427-435

[6] G. Shin, M.Y. Bae, H. J. Lee, S.K. Hong, C.H. Yoon, G. Zi, J.A. Rogers, J.S. Ha Acs Nano 5 (12) 2011, 10009-10016.

[7] L. Guo, E. Leobandung, S.Y. Chou, Appl. Phys. Lett. 70 (1997) 850.

[8] R. Cooper, H.P. Upadhyaya, T.K. Minton, M. R. Berman, X. Du, S.M. George, Thin Solid Films 516 (2008) 4036–4039

[9] S. Raghu, S. B. Chung , S. Lederer, Journal of Physics: Conference Series 449(2013) 012031.

[10] W. Oelerich, T. Klassen, R. Bormann, J. Alloys Compd. 315 (2001) 237–242.

[11] (a) C. Wang, L. Yin , L. Zhang, D. Xiang, R. Gao Sensors10 (2010) 2088-2106. (b)G. Korotcenkov. Mater. Sci. Eng. B 139 (2007) 1–23.

[12] V. Balouria, S. Samanta, A. Singh, A.K. Debnatha, A. Mahajan, R.K. Bedi, D.K. Aswal, S.K. Gupta, Sens. Actuators B: Chem. 176 (2013) 38–45.

[13] V. Srikant, D. R. Clarke, J. Appl. Phys. 83 (1998).

[14] F. M. Li, G. W. Hsieh, S. Dalal, M. C. Newton, J. E. Stott, P. Hiralal, A. Nathan, P. A. Warburton, H. E. Unalan, P. Beecher, A. J. Flewitt, I. Robinson, G. Amaratunga, W. I. Milne, IEEE Trans. Electron Dev. 55 (2008) 3001.

[15] Y. Dan, Y. Cao, T. E. Mallouk, S. Evoy, A. T. C. Johnson, Nanotechnology 20 (2009) 434014-4.

[16] M. Yun, C. Lee, R. P. Vasquez, R. Penner, M. Bangar, A. Mulchandani, N. V. Myung, Proc. SPIE 5593 (2004) 200-206.

[17] R. A. Michaels, Environ. Health Persp. 107 (1999) 617-627.

[18] P. G. Su, C. T. Lee, C. Y. Chou, K. H. Cheng, Y. S. Chuang, Sens. Actuators B: Chem. 139 (2009) 488-493.

[19] X. Wang, C. J. Summers, Z. L. Wang, Nano Lett. 4 (2004) 423-426.

[20] L. E. Greene, M. Law, J. Goldberger, F. Kim, J. C. Johnson, Y. Zhang, R. J. Saykally, P. Yang, Angew. Chem. Int. Ed. 42 (2003) 3031-3034.

[21] W. Z. Liu, H. Y. Xu, L. Wang, X. H. Li, Y. C. Liu, AIP Adv. 1 (2011) 022145-8.

[22] L. Vayssieres, Adv. Mater. 15 (2003) 464-466.

[23] X. W. Sun, J. Z. Huang, J. X. Wang, Z. Xu, Nano Lett. 8 (2008) 1219-1223.

[23] P. Wu, H. Zhang,Y. Qian,Y. Hu, H. Zhang, C. Cai, J. Phys. Chem. C 117 (2013), 19091−19100.

[24] X. Zhao, Y. Wu, X. Hao, Int. J. Electrochem. Sci. 8 (2013) 1903 –1910.

[25] X. T. Hoang, D. T. Nguyen, B. C. Dong, H. N. Nguyen, Adv. Nat. Sci.: Nanosci. Nanotechnol. 4 (2013) 035013.

[26] M. A. Zeeshan, S. Pane, S. K. Youn , E. Pellicer, S. Schuerle, J. Sort, S. Fusco, A. M. Lindo, H. G. Park, B. J. Nelson, Adv. Funct. Mater. 23 (2013) 823–831.

[27] F. I. Dar, K. R. Moonooswamy, M. Es-Souni, Nanoscale Res. Lett. 8:363 (2013).

[28] X. Zhao, G. Meng, F. Han, X. Li, B. Chen, Q. Xu, X. Zhu, Z. Chu, M. Kong, Q. Huang, Sci. Rep. 3: 2238 (2013).

[29] N. S. Ramgir, Y. Yang, M. Zacharias, Small 6 (2010) 1705-1722.

[30] C. S. Rout, S. H. Krishna, S. R. C. Vivek chand, A. Govindaraj, C.N.R. Rao, Chem. Phys. Lett. 418 (2006) 586-590.

[31] M. H. Huang, S. Mao, H. Feick, H. Q. Yan, Y. Y. Wu, H. Kind, E. Weber, R. Russo, P. Yang, Science 292 (2001) 1897-1899.

[32] N. Riehl, O. Z. Ortman, Electrochem. 60 (1952) 149.

[33] P. H. Kasai, Phys. Rev. 130 (1963) 989.

[34] F. A. Kroger, H. J. Vink, J. Chem. Phys. 22 (1954) 250.

[35] I. Y. Prosanov, A. A. Politov, Inorg. Mater. 31 (1995) 663.

[36] D. Hahn, R. Nink, Phys. Condens. Mater. 3 (1965) 311.

[37] M. Liu, A. H. Kitai, P. J. Mascher, Lumin. 54 (1992) 35.

[38] E. G. Bylander, J. Appl. Phys. 49 (1978) 1188.

[39] C. S. Rout, M. Hegde, A. Govindaraj, C.N.R. Rao, Nanotechnology 18 (2007) 2055041–2055049.

[40] D. R. Patil, L. A. Patil, IEEE Sens. J. 7 (2007) 434-439.

[41] B. Timmer, W. Olthuis, A. van den Berg, Sensors and Actuators B: Chem. 107 (2005) 666–677.

[42] M. S. Wagh, G. H. Jain, D. R. Patil, S. A. Patil, L. A. Patil, Sensors and Actuators B: Chem. 115 (2006) 128-133.

[43] B. Karunagaran, P. Uthirakumar, S. J. Chung, S. Velumani, E. -K. Suh, Mater. Charact. 58 (2007) 680–684.

[44] N. Kumar, G. D. Varma, R. Nath, A. K. Srivastava, Appl. Phys. A 104 (2011) 1169-1174.

[45] B. K. Gupta, V. Grover, G. Gupta, V. Shanker, Nanotechnology 21 (2010) 475701.

[46] M. Wu, L. Yao, W. Cai, G. Jiang, X. Li, Z. Yao, J. Mater. Sci. Technol. 10 (2004) 11-13.

[47] H. A. Pohl, J. Appl. Phys. 22 (1951) 869-3.

[48] D. Q. Wang, R. Zhu, Z. Y. Zhou, X. Y. Ye, Chin. Phys. B 17 (2008) 3875-3879.

[49] V. Srikant D. R. Clarke, J. Appl. Phys. 83 (1998) 5447-5.

[50] N. S. Ramgir, M. Ghosh, P. Veerender, N. Datta, M. Kaur, D. K. Aswal, S. K. Gupta, Sens. Actuators B: Chem. 156 (2011) 875-880.

[51] N. Yamazoe, K. Shimanoe, Sens. Actuators B: Chem. 128 (2008) 566-573.

[52] J. C. Belmonte, J. Manzano, J. Arbiol, A. Cirera, J. Puigcorbe, A. Vila, N. Sabate, I. Gracia, C. Cane J. R. Morante, Sens. Actuators B: Chem. 114 (2006) 881-892.

[53] O. Lupan, L. Chow, T. Pauporte, L. K. Onoa, B. Roldan Cuenya, G. Chai, Sens. Actuators B: Chem. 173 (2012) 772– 780.

[54] Z. Yang, L. M. Li, Q. Wan, Q. H. Liu, T. H. Wang, Sens. Actuators B: Chem. 135 (2008) 57-60.

[55] Y. Mas, W. L. Wang, K. J. Liao, C.Y. Kong, J. Wide Bandgap. Mater. 10 (2002) 113-119.

[56] P. Feng, Q. Wan, T. H. Wang, Appl. Phys. Lett. 87 (2005) 213111-3.

Table of contents entry

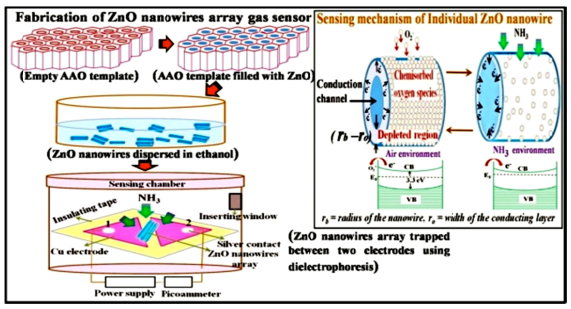

Demonstrations of highly ordered luminescent ZnO nanowires array were synthesized which has excellent sensitivity and fast response to NH_3 gas.

Table of contents entry

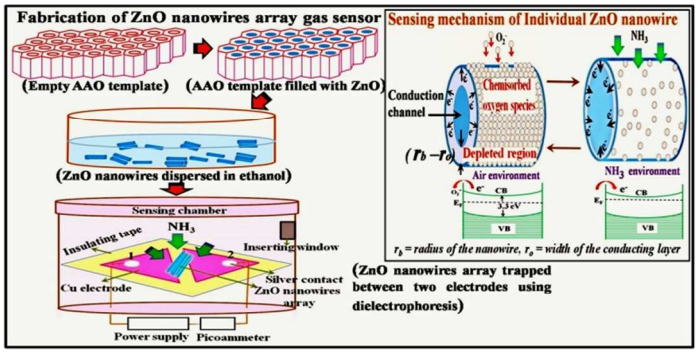

Demonstrations of highly ordered luminescent ZnO nanowires array were synthesized which has excellent sensitivity and fast response to NH_3 gas.